Electronic Supplementary Material (ESI)

Supramolecular Arrays by Self-assembly of Terpyridine-Based Monomers with Transition Metal Ions

Ting-Zheng Xie,[a] Yuchen Yao,[a] Xinyu Sun,[a] Kevin J. Endres,[b] Shiying Zhu,[a] Xiaolei Wu,[a] Hui Li,[a] James M. Ludlow III,[c] Tianbo Liu,[a] Min Gao,[d] Charles N. Moorefield,[e] Mary Jane Saunders,[f] Chrys Wesdemiotis,*[,a,b] George R. Newkome*[,a,b,g]

[a]Department of Polymer Science and [b]Department of Chemistry, The University of Akron, Akron, Ohio 44256 United States
[c]Saint-Gobain, 2664 Gilchrist Rd, Akron, Ohio 44305 United States
[d]Liquid Crystal Institute, Kent State University, Kent, Ohio 44242 United States
[e]Dendronex LLC, 109 Runway Drive, Lubbock, Texas 79416 United States
[f]Department of Biological Sciences, Florida Atlantic University, Boca Raton, Florida 33431 United States
[g]Center for Molecular Biology and Biotechnology, Florida Atlantic University, 5353 Parkside Dr., Jupiter, FL 33458 United States

TABLE OF CONTENTS

Experimental Section.

General Procedures. Chemicals were commercially purchased and used without further purification. Thin layer chromatography (TLC) was conducted on flexible sheets (Baker-flex) precoated with Al_2O_3 (IB-F) or SiO_2 (IB2-F) and visualized by UV light. Column chromatography was conducted using basic Al_2O_3, Brockman Activity I (60-325 mesh) or SiO_2 (60-200 mesh) from Fisher Scientific.

The NMR spectra were recorded on either a Varian Mercury 300 or Varian NMRS 500 spectrometer, using CD_3CN for the complexes and $CDCl_3/CD_3OD$ for the ligands, except where otherwise noted. Mass spectra were obtained on a Synapt HDMS quadrupole/time-of-flight (Q/TOF) mass spectrometer (Waters Corp., Milford, MA) and a Bruker Esquire electrospray ion trap mass spectrometer (ESI-MS). The Synapt Q/ToF instrument contains a traveling wave ion mobility (TWIM) device in which ions drift under the influence of a traveling wave field against the flow of the carrier gas (N_2). This process disperses the ions, based on their mass, charge, and shape (architecture). The separated ions travel through the transfer cell from which they are conveyed to the orthogonal ToF analyzer for *m/z* measurement. The acquired data are typically displayed in 2D plots of *m/z* ratio *vs*. the corresponding drift time through the IM cell. The TWIM MS experiments were performed under the following conditions: ESI capillary voltage, 1 kV; sample cone voltage, 8 V; extraction cone voltage, 3.2 V; desolvation gas flow, 800 L/h (N_2); trap collision energy (CE), 3 eV; transfer CE, 1 eV; trap gas flow, 1.5 mL/min (Ar); TWIM cell gas flow, 22.7 mL/min (N_2); sample flow rate, 5 μL/min; source temperature, 20 °C; desolvation temperature, 40 °C; TWIM wave height, 7.5 V; and TWIM wave velocity, 350 m/s. TWIM data analyses were conducted using the MassLynx 4.1 and DriftScope 2.1 programs provided by Waters. For the TEM investigation, the sample was dissolved in DMF : H_2O = 5 : 1 at a concentration within the range 10^{-3} to 10^{-4} M. The solutions were drop cast onto a carbon-coated copper grid and the excess solvent was absorbed by filter paper to avoid aggregation. The TEM images of these samples were taken with a Jeol JEM-1230 transmission electron microscope. The AFM (atomic force microscopy) was performed using a Bruker Dimension Icon in Scanasyst mode, with a Scanasyst-Air cantilever (spring constant 0.2–0.8 N m^{-1}) in air. The samples were spin coated onto the silicon wafer and left to dry under ambient conditions. Silicon substrates were cleaned using the well-known Piranha method followed by sonication in DI water for 15 minutes.

Collision cross-section calibration. The drift time scale of the TWIM-MS experiments was converted to a collision cross-section (CCS) scale, following the calibration procedure of Scrivens *et al*.[S1] The calibration curve was constructed by plotting the corrected CCSs of the molecular ions of insulin (bovine pancreas), ubiquitin (bovine red blood cells), lysozyme, and cytochrome C (horse heart)[S2] against the corrected drift times (arrival times) of the corresponding molecular ions measured in TWIM-MS experiments at the same traveling wave velocity, traveling wave height, and ion mobility gas flow settings used for the metallo-macrocycles, *viz*. 350 m/s, 7.5 V,

and 22.7 mL/min, respectively.

Molecular modeling. Energy minimization of the macrocycles was conducted with the Materials Studio program, version 4.2, using the Anneal and Geometry Optimization tasks in the Forcite module (Accelrys Software, Inc.). All counterions were omitted. An initially energy-minimized structure was subjected to 100 annealing cycles with initial and mid-cycle temperatures of 300 and 1500 K, respectively, twenty heating ramps per cycle, one thousand dynamic steps per ramp, and one dynamic step per femtosecond. The constant volume/constant energy (NVE) ensemble was used and the geometry was optimized after each cycle. Geometry optimization used a universal force field with atom-based summation and cubic spline truncation for both the electrostatic and van der Waals parameters.

4'-(4-Boronatophenyl)[2,2':6',2'']terpyridine (**2**) was prepared from 4-formylphenylboronic acid by a known procedure:[S3] m.p. >300 °C.

4',4''''-{4',5'-*Bis*(docosyloxy)[1,1':2',1''-terphenyl]-4,4''-diyl}di[2,2':6',2'']-terpyridine (3) was prepared by a known procedure[S4] affording (66%) ligand **3**, as a white solid: 3.11 g, m.p. > 300 °C; ^{1}H NMR ($CDCl_3$, 500 MHz): δ 8.78 (s, 4H, 3',5'-tpy*H*), 8.71-8.72 (d, 4H, *J* = 4 Hz, 3,3''-tpy*H*), 8.67-8.68 (d, 4H, *J* = 8 Hz, 6,6''-tpy*H*), 7.84-7.89 (t, 4H, 4,4''-tpy*H*), 7.83-7.84 (d, 4H, *J* = 8 Hz, Ph'*H*), 7.32-7.36 (m, 8H, 5,5''-tpy*H*, Ph'*H*), 7.04 (s, 2H, Ph*H*), 4.11-4.14 (t, 4H, 2 × CH_2), 1.87-1.90 (q, 4H, 2 × CH_2), 1.51-1.54 (q, 4H, 2 × CH_2), 1.26-1.40 (m, 72H, 36 × CH_2), 0.87-0.89 (t, 6H, 2 × CH_3) (**Fig. S1**); ^{13}C NMR (500 MHz, $CDCl_3$, ppm): δ 146.02, 144.85, 144.77, 138.52, 133.29, 132.09, 128.65, 126.59, 123.05, 119.86, 117.60, 115.11, 112.36, 73.30, 73.05, 72.79, 65.68, 25.75, 25.52, 25.46, 22.15, 18.73 (**Fig. S2**); MALDI-MS (*m/z*): 1341.9627 [M^+] (calcd *m/z* = 1342.0120) (Fig. S3).

[(Ru^{2+})(3)$_2$(Cl^-)$_2$] (4) was prepared by a known procedure[S4] generating the desired **4**, isolated as a red powder: 1.52 g (50%); m.p. >300°C; ^{1}HNMR (500 MHz, 1:2 CD_3OD:$CDCl_3$): δ 9.07 (s, 4H, complexed 3',5'-tpy*H*), 8.73-8.75 (d, 4H, *J* = 8 Hz, complexed 3,3''-tpy*H*), 8.65 (s, 4H, free 3',5'-tpy*H*), 8.63-8.65 (m, 8H, free 3,3''-tpy*H* and free 6,6''-tpy*H*), 8.06-8.08 (d, 4H, *J* = 8 Hz, complexed Ph*H*), 7.91-7.94 (m, 8H, complexed and free 4,4''-tpy*H*), 7.84-7.86 (d, 4H, *J* = 7 Hz, free Ph*H*), 7.51-7.53 (d, 4H, *J* = 8 Hz, free Ph*H*), 7.43-7.44 (m, 4H, free 5,5''-tpy*H*), 7.38-7.40 (m, 8H, complexed Ph*H*), 7.34-7.35 (d, 4H, *J* = 6 Hz, complexed 6,6''-tpy*H*), 7.19-7.22 (t, 4H, complexed 5,5''-tpy*H*), 7.11 (s, 2H, complexed Ph*H*), 7.08 (s, 2H, free Ph*H*), 4.13-4.17 (q, 8H, complexed and free 4 × CH_2), 1.88-1.89 (m, 8H, complexed and free 4 × CH_2), 1.54-1.56 (m, 8H, complexed and free 4 × CH_2), 1.31-1.40 (m, 8H, complexed and free 4 × CH_2), 1.18-1.33 (m, 136H, complexed and free 34 × CH_2), 0.83-0.86 (t, 12H, complexed and free 4 × CH_3) (**Fig. S4**); 2D ^{1}H-^{1}H COSY NMR (500 MHz, $CDCl_3$) (**Fig. S5**); ^{13}C NMR (500 MHz, $CDCl_3$, ppm): δ 157.95, 155.20, 151.69, 149.22, 148.92, 148.29, 144.32, 142.76, 138.46, 133.86, 132.88, 131.97, 131.32, 130.80, 127.95, 126.84, 124.97, 124.46, 122.21, 118.89, 116.46, 116.35, 77.30, 69.91, 69.67,

48.54, 31.80, 29.59, 29.35, 29.22, 26.07, 26.03, 22.53, 13.76 (**Fig. S6**); MALDI-MS (*m/z*): 2785.7617 (calcd m/z = 2785.0940) (**Fig. S7**).

[$(Ru^{3+})_2$ (4)$(Cl^-)_8$] (5) was prepared by a known procedure[S4] to give (93%) **5**, as a red powder (321 mg), which was used directly without further purification: MALDI-MS (*m/z*): 3235.5828 (calcd *m/z* = 3235.3840) (**Fig. S8**).

[$(Ru^{2+})_2$(5)(2,3,6,7-Tetra*kis*(4-terpyridinylphenyl)-9,10-dimethyl-9,10-ethanoanthracene)$(Cl^-)_6$] (7): To a 1L round bottom flask, **5** (286 mg, 100 μmol), 2,3,6,7-tetra*kis*(4-terpyridinylphenyl)-9,10-dimethyl-9,10-ethanoanthracene[S7] (176 mg, 120 μmol), $CHCl_3$ (150 mL), MeOH (150 mL), and 4-ethylmorpholine (2 mL) were added. After refluxing for 24 h at 80 °C, the reaction was concentrated *in vacuo* to give a red powder, which was purified by column chromatography (Al_2O_3, $CHCl_3$ → 16:1 $CHCl_3$:MeOH) to remove free **5** and free 2,3,6,7-tetra*kis*(4-terpyridinylphenyl)-9,10-dimethyl-9,10-ethanoanthracene to give (56%) the desired **7**, as a red powder: 259 mg, m.p. > 300°C; ^{1}H NMR (500 MHz, 1:2 CD_3OD:$CDCl_3$): δ 9.20 (s, 12H, complexed 3',5'-tpy*H*), 8.88-8.90 (m, 12H, complexed 3,3"-tpy*H*), 8.60-8.65 (m, 12H, free 3',5'-tpy*H*, free 3,3"-tpy*H*, and free 6,6"-tpy*H*), 8.15-8.16 (m, 12H, complexed Ph*H*), 7.89-7.92 (t, 12H, complexed 4,4"-tpy*H*), 7.85-7.86 (d, 4H, *J* = 8 Hz, free Ph*H*), 7.63 (s, 2H, free Ph*H*), 7.54-7.60 (m, 12H, complexed Ph*H*), 7.43 (m, 4H, free 6,6"-tpy*H*), 7.41 (m, 4H, free Ph*H*), 7.40 (m, 4H, free 4,4"-tpy*H*), 7.20-7.22 (t, 12H, complexed 5,5"-tpy*H*), 7.17 (s, 6H, complexed Ph*H*), 4.18-4.20 (t, 8H, 4 × CH_2), 2.23 (s, 6H, 2 × CH_3), 1.15-1.43 (m, 136H, 68 × CH_2), 0.84-0.86 (t, 12H, 4 × CH_3) (**Fig. S9**); 2D ^{1}H-^{1}H NOESY NMR (500 MHz, 300K, CD_3OD:$CDCl_3$ (1:2) (**Fig. S10**); ^{13}C NMR (500 MHz, 1:2 CD_3OD:$CDCl_3$, ppm): δ = 158.05, 155.21, 151.70, 148.85, 138.36, 131.26, 127.84, 127.57, 121.59, 111.15, 77.54, 77.28, 77.02, 74.99, 74.83, 69.23, 62.31, 62.27, 61.97, 49.08, 48.40, 36.89, 33.96, 31.80, 31.61, 29.42, 26.11, 25.17, 25.13, 24.73, 22.53, 22.42, 20.93, 20.31, 13.78, 13.71 (**Fig. S11**); ESI-MS (*m/z*): 1519 [**5**-3Cl^-]$^{3+}$ (calcd *m/z* = 1519.037), 1130 [**7**-4Cl^-]$^{4+}$ (calcd *m/z* = 1130.403), 897 [**7**-5Cl^-]$^{5+}$ (calcd *m/z* = 897.222), 742 [**7**-6Cl^-]$^{6+}$ (calcd *m/z* = 741.768) (**Fig. S16**).

[$(Zn^{2+})_3$(7)$_3$$(PF_6^-)_{24}$] (8): To a 25 mL round bottom flask, **7** (24 mg, 5.2 μmol), $Zn(NO_3)_2$·$6H_2O$ (1.84 mg, 6.2 μmol), $CHCl_3$ (6 mL), and MeOH (6 mL) were added. After stirring at 20 °C for 5 h, NH_4PF_6 (67 mg, 411 μmol) was added. After stirring at 20 °C for another 12 h, a red precipitate formed and the solvent became transparent. The red precipitate was filtered *in vacuo*, washed several times with H_2O and MeOH to remove excess **7**, $Zn(NO_3)_2$·$6H_2O$ and NH_4PF_6 to give **8** (PF_6^-), as a red powder: 21 mg (87%); m.p. > 300°C; ^{1}H NMR (500 MHz, 300 K, 1:2 CD_3OD:$CDCl_3$): δ = 8.55-8.57 (m, 48H, 3',5'-tpy*H*), 8.25 (m, 12H, Zn coordinated 5,5"-tpy*H*), 8.18 (m, 48H, 3,3'-tpy*H*), 7.60 (m, 24H, Ph*H* on tetra*kis*tpy), 7.55 (m, 24H, Ph*H* on tetra*kis*tpy), 7.45 (m, 12H, Ph*H* on *bis*tpy), 7.22 (m, 48H, 4,4'-tpy*H*), 7.04-7.09 (m, 12H, Zn coordinated 6,6"-tpy*H*), 7.00-7.01 (m, 24H, Ph*H* on tetra*kis*tpy), 6.93-6.94 (d, 24H, *J* = 7.7 Hz, Ph*H* on *bis*tpy), 6.86 (m, 36H, Ru coordinated 6,6"-tpy*H*), 6.59 (s, 12H, Ph*H* on *bis*tpy),

6.49-6.50 (t, 36H, Ru coordinated 5,5"-tpy*H*), 3.55 (t, 24H, 12 × CH_2), 2.11 (s, 18H, 6 × CH_3), 1.50-1.53 (m, 12H, 6 × CH_2), 1.20-1.23 (m, 24H, 12 × CH_2), 0.90-0.93 (m, 24H, 12 × CH_2), 0.51-0.78 (m, 432H, 216 × CH_2), 017-0.19 (t, 36H, 12 × CH_3) (**Fig. S12**); ESI-MS (*m/z*): 2288 [**8**-7PF_6^-]$^{7+}$ (calcd *m/z* = 2287.604), 1984 [**8**-8PF_6^-]$^{8+}$ (calcd *m/z* = 1983.354), 1747 [**8**-9PF_6^-]$^{9+}$ (calcd *m/z* = 1747.034), 1558 [**8**-10PF_6^-]$^{10+}$ (calcd *m/z* = 1557.835), 1403 [**8**-11PF_6^-]$^{11+}$ (calcd *m/z* = 1403.035), 1274 [**8**-12PF_6^-]$^{12+}$ (calcd *m/z* = 1274.036), 1165 [**8**-13PF_6^-]$^{13+}$ (calcd *m/z* = 1164.882), 1071 [**8**-14PF_6^-]$^{14+}$ (calcd *m/z* = 1071.322), 990 [**8**-15PF_6^-]$^{15+}$ (calcd *m/z* = 990.237), and 919 [**6**-16PF_6^-]$^{16+}$ (calcd *m/z* = 919.287) (**Fig. S13** is Fig. 3 in manuscript); 2D ^{1}H-^{1}H COSY NMR (500 MHz, 300 K, 1:2 $CDCl_3$:CD_3CN) (**Fig. S14**); AFM (**Fig. S18**); DLS plot (1.2 mg/mL) (**Fig. S19**); UV-vis monomer: (500 μg, DMF) and assembly [500 μg, DMF:H_2O (5:1, v/v)] (**Fig. S20**).

[(Zn^{2+})$_3$(7)$_3$(BPh_4^-)$_{24}$] (9): To a 25 mL round bottom flask, **7** (24 mg, 5.2 μmol) $Zn(NO_3)_2{\cdot}6H_2O$ (1.84 mg, 6.2 μmol), $CHCl_3$ (6 mL), and MeOH (6 mL) were added, then after stirring at 20 °C for 5 h, $NaBPh_4$ (28 mg, 411 μmol) was added. After stirring at 20 °C for another 12 h, a red precipitate formed along with transparent solvent. The precipitate was filtered *in vacuo* and washed with H_2O and MeOH to remove free **5**, $Zn(NO_3)_2{\cdot}6H_2O$, and $NaBPh_4$ to afford **9**, as a red powder: 20 mg (83%); ^{1}H NMR (500 MHz, 1:2 CD_3OD:$CDCl_3$): δ = 9.45-9.57 (m, 48H, 3',5'-tpy*H*), 9.25 (m, 12H, Zn coordinated 5,5"-tpy*H*), 9.18 (m, 48H, 3,3'-tpy*H*), 8.60 (m, 24H, Ph*H* on tetra*kis*tpy), 8.55 (m, 24H, Ph*H* on tetra*kis*tpy), 8.45 (m, 12H, Ph*H* on *bis*tpy), 8.22 (m, 48H, 4,4′-tpy*H*), 8.04-8.09 (m, 12H, Zn coordinated 6,6"-tpy*H*), 8.00-8.01 (m, 24H, Ph*H* on tetra*kis*tpy), 7.93-7.94 (d, 24H, *J* = 7.7 Hz, Ph*H* on *bis*tpy), 7.86 (m, 36H, Ru coordinated 6,6"-tpy*H*), 7.59 (s, 12H, Ph*H* on *bis*tpy), 7.49-7.50 (t, 36H, Ru coordinated 5,5"-tpy*H*), 7.16 (d, 192H, Ph*H* on BPH_4^-), 6.90-6.87 (t, 192H, Ph*H* on BPH_4^-), 6.90-6.87 (t, 96H, Ph*H* on BPH_4^-), 4.19 (t, 24H, 12 × CH_2), 3.11 (s, 18H, 6 × CH_3), 1.89-1.91 (m, 12H, 6 × CH_2), 1.40-1.42 (m, 24H, 12 × CH_2), 1.34-1.36 (m, 24H, 12 × CH_2), 1.22-1.26 (m, 432H, 216 × CH_2), 0.82-0.85 (t, 36H, 12 × CH_3) (**Fig. S15**); molecular weight: 14648.42; ESI-MS (*m/z*): 3216 [**9**-6BPh_4^-]$^{6+}$ (calcd *m/z* = 3215.81), 2711 [**9**-7BPh_4^-]$^{7+}$ (calcd *m/z* = 2710.81), 2332 [**9**-8BPh_4^-]$^{8+}$ (calcd *m/z* = 2332.05), 2037 [**9**-9BPh_4^-]$^{9+}$ (calcd *m/z* = 2037.46), 1802 [**9**-10BPh_4^-]$^{10+}$ (calcd *m/z* = 1801.80), 1609 [**9**-11BPh_4^-]$^{11+}$ (calcd *m/z* = 1608.97) (**Fig. S17**).

NMR spectra of ligand and complexes.

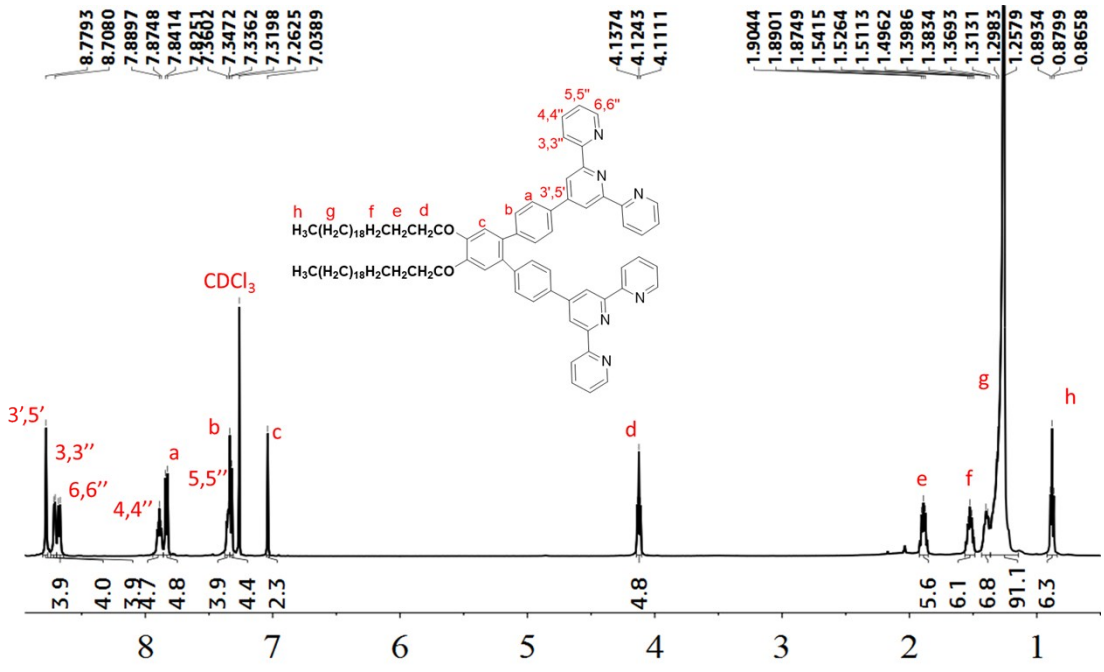

Figure S1. ^{1}H NMR spectrum (500 MHz, 300 K) of **3** in $CDCl_3$.

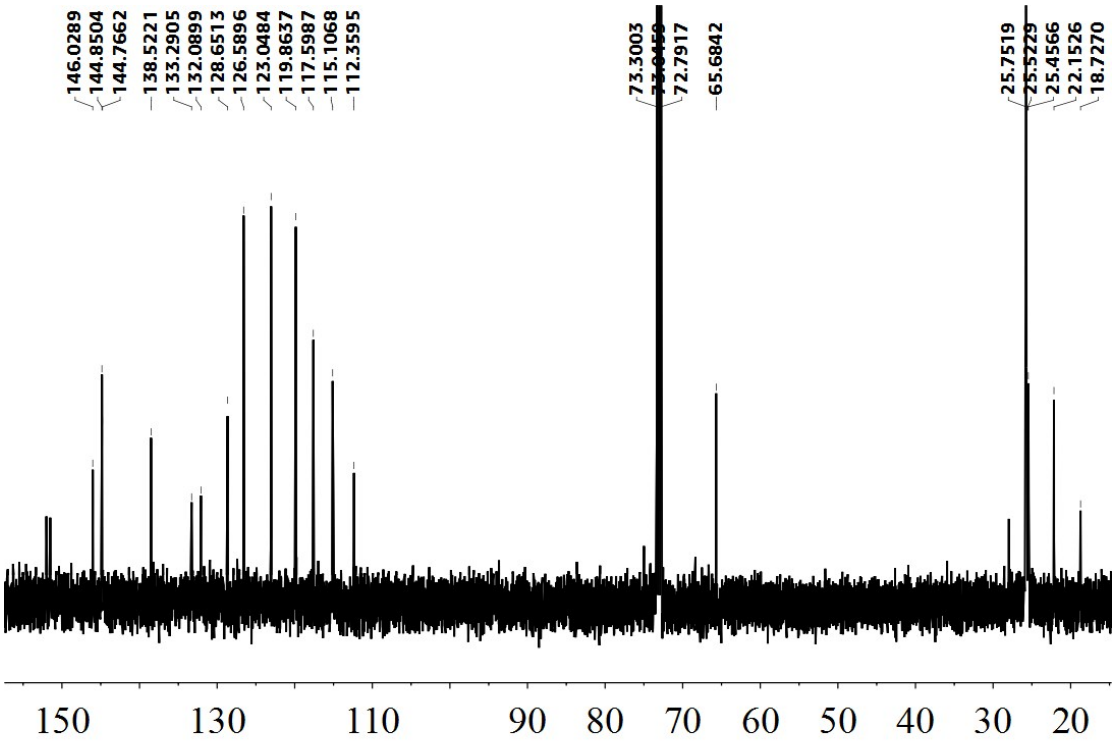

Figure S2. ^{13}C NMR spectrum (500 MHz, 300 K) of **3** in $CDCl_3$.

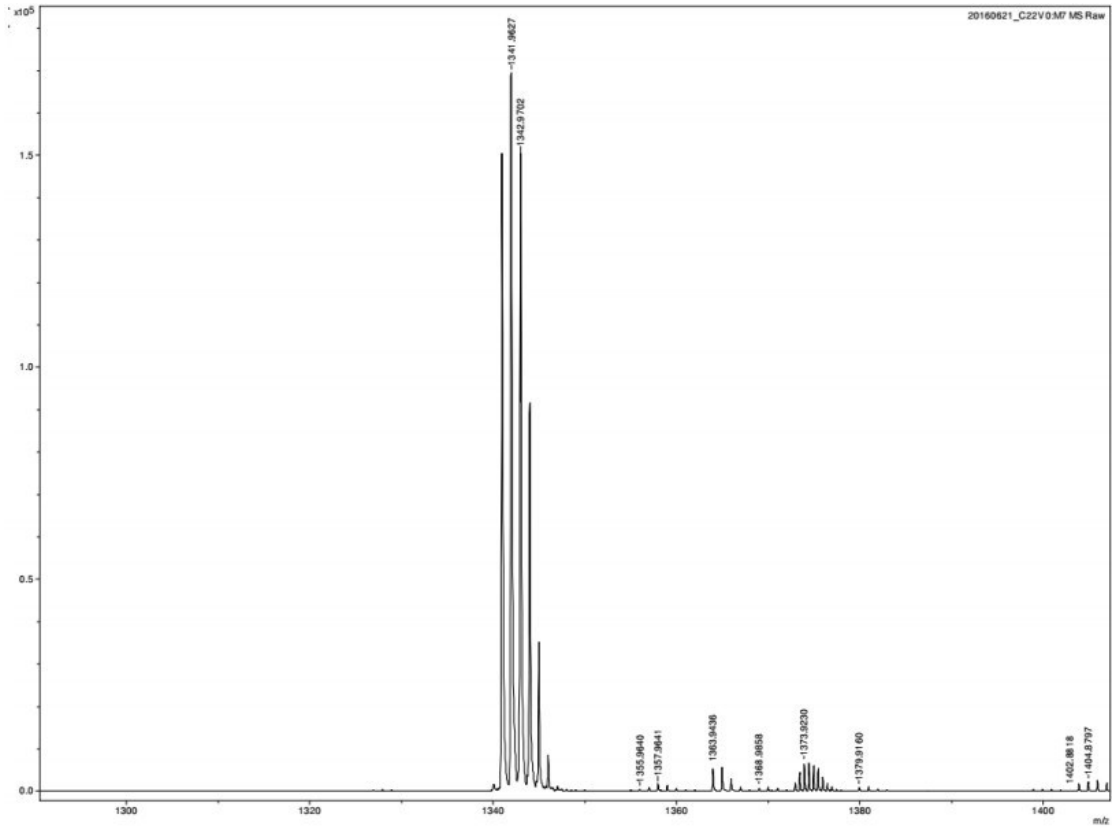

Figure S3. MALDI-MS spectrum of ligand **3**.

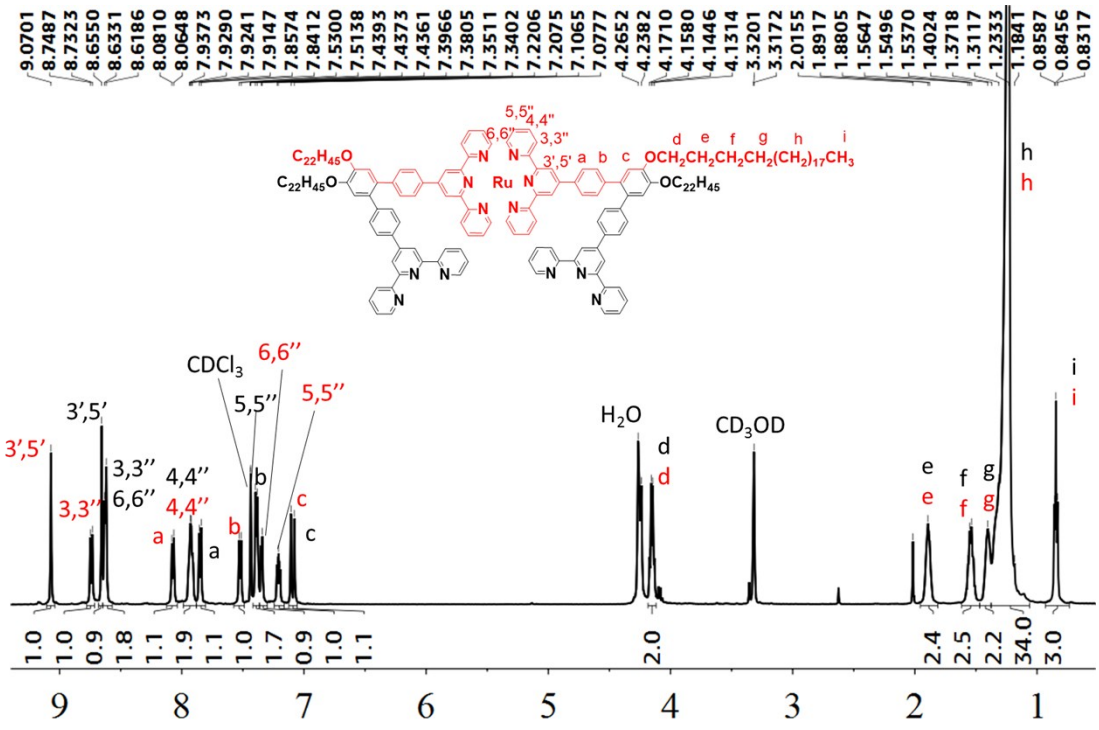

Figure S4. ^{1}H NMR spectrum (500 MHz, 300 K) of **4** in $CDCl_3/CD_3OD$ (2:1, v/v).

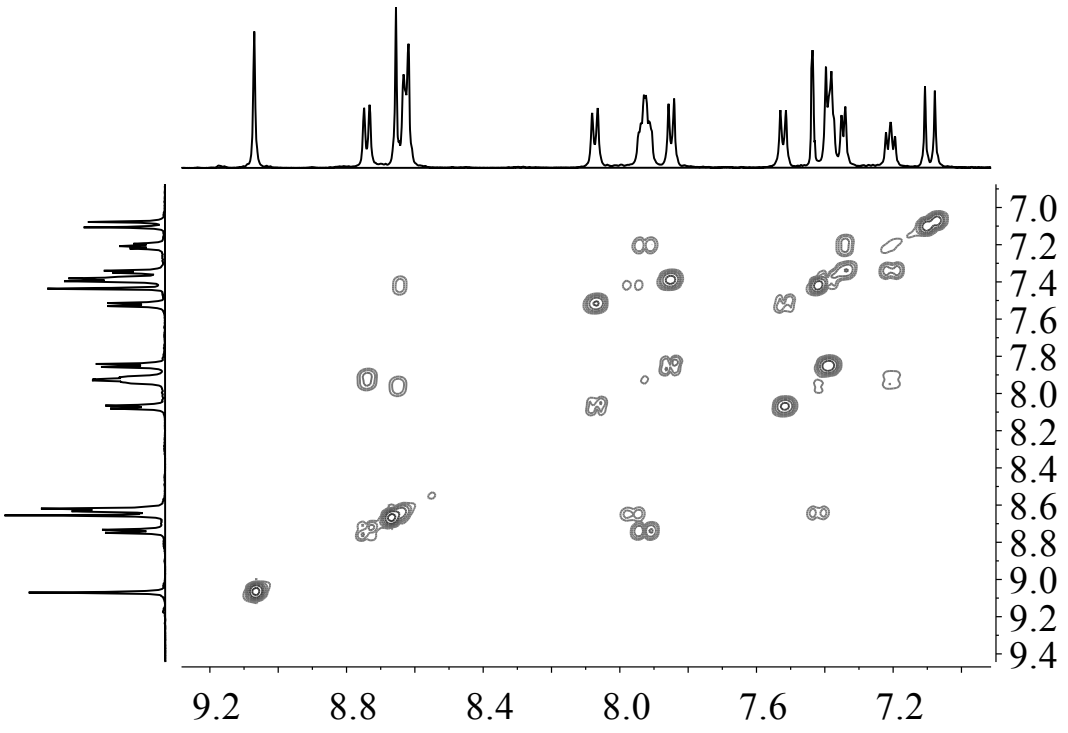

Figure S5. 2D ^{1}H-^{1}H COSY NMR spectrum (500 MHz, 300 K) of **4** in $CDCl_3$.

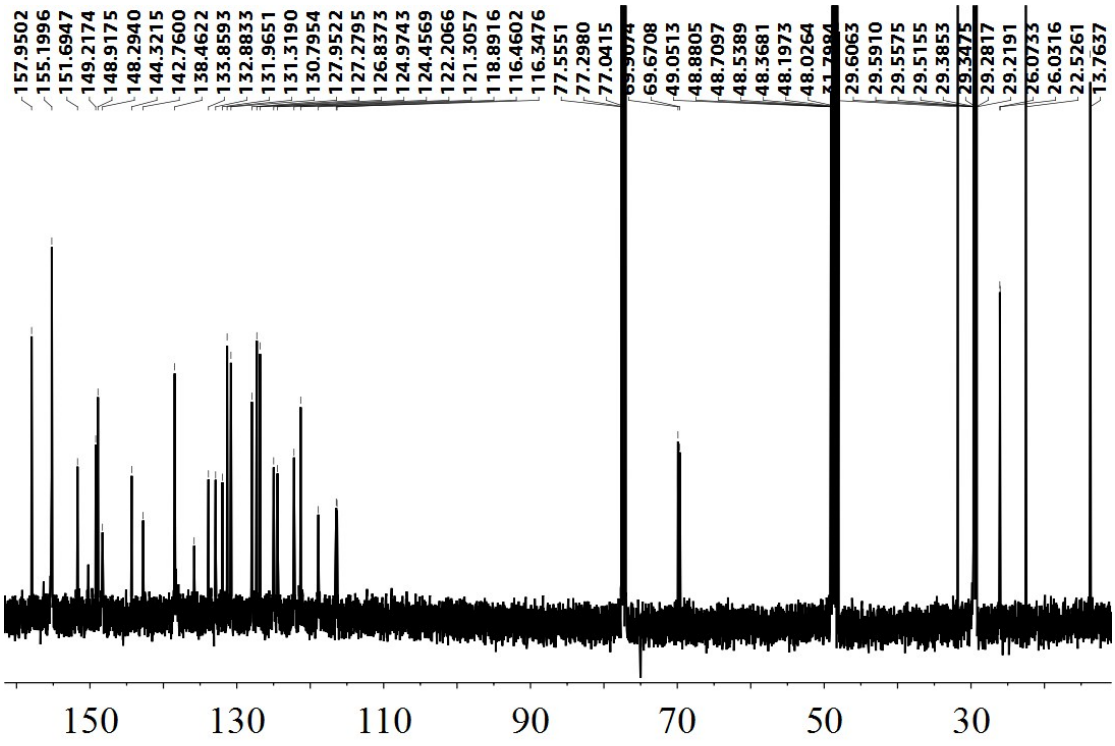

Figure S6. ^{13}C NMR spectrum (500 MHz, 300 K) of **4** in $CDCl_3$.

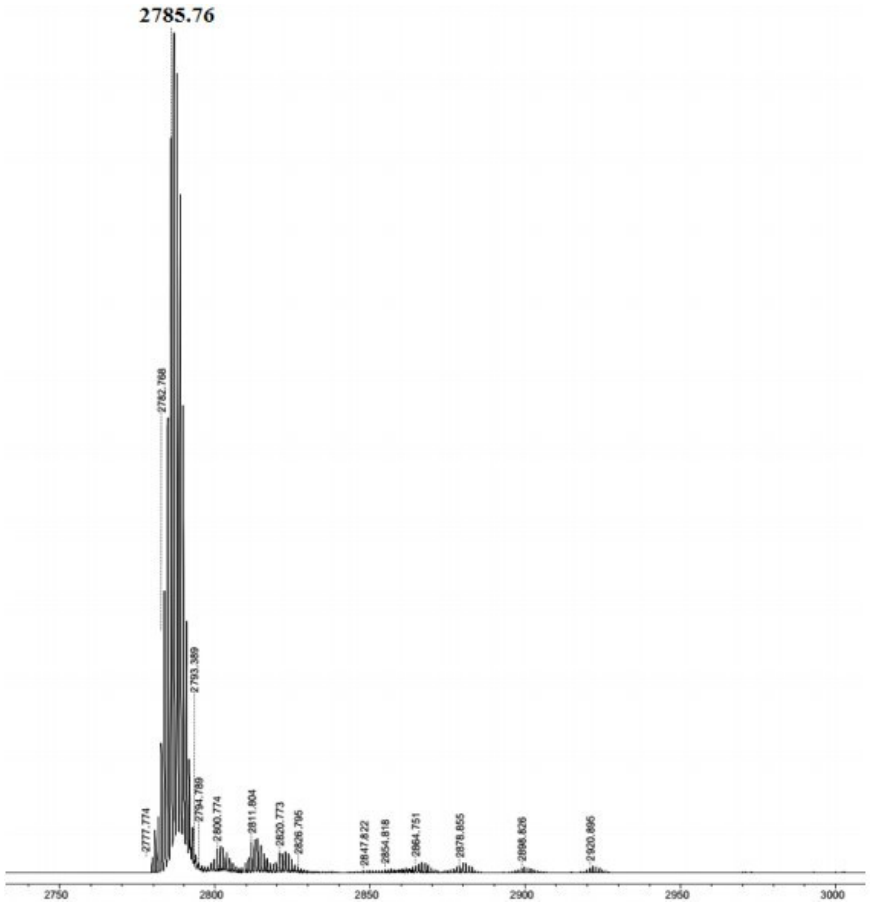

Figure S7. MALDI-MS spectrum of complex **4**.

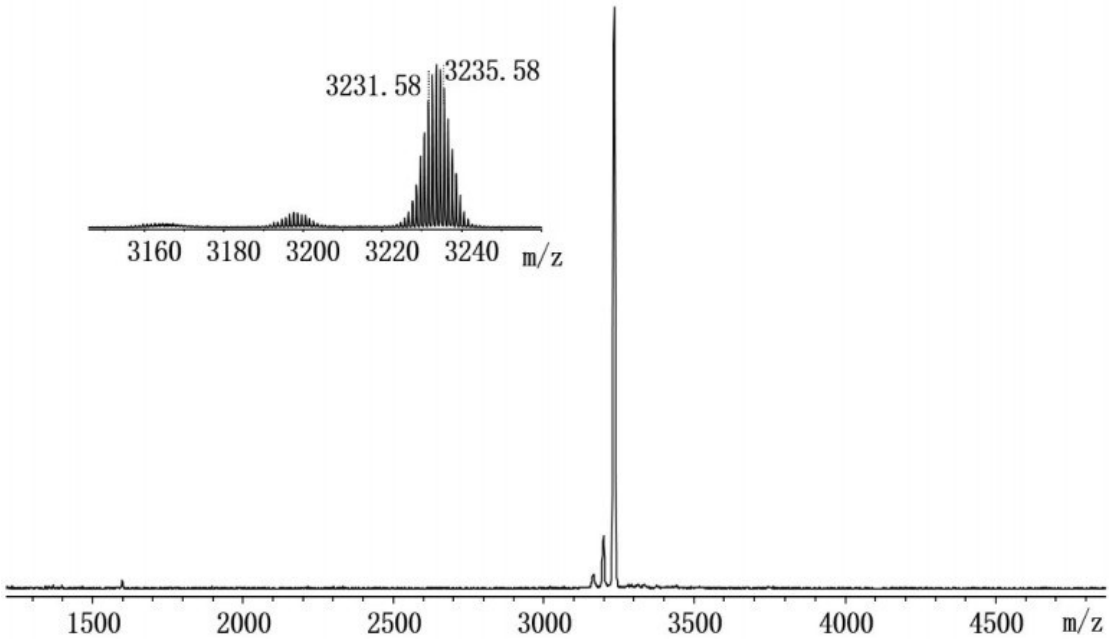

Figure S8. MALDI-MS spectrum of complex **5**.

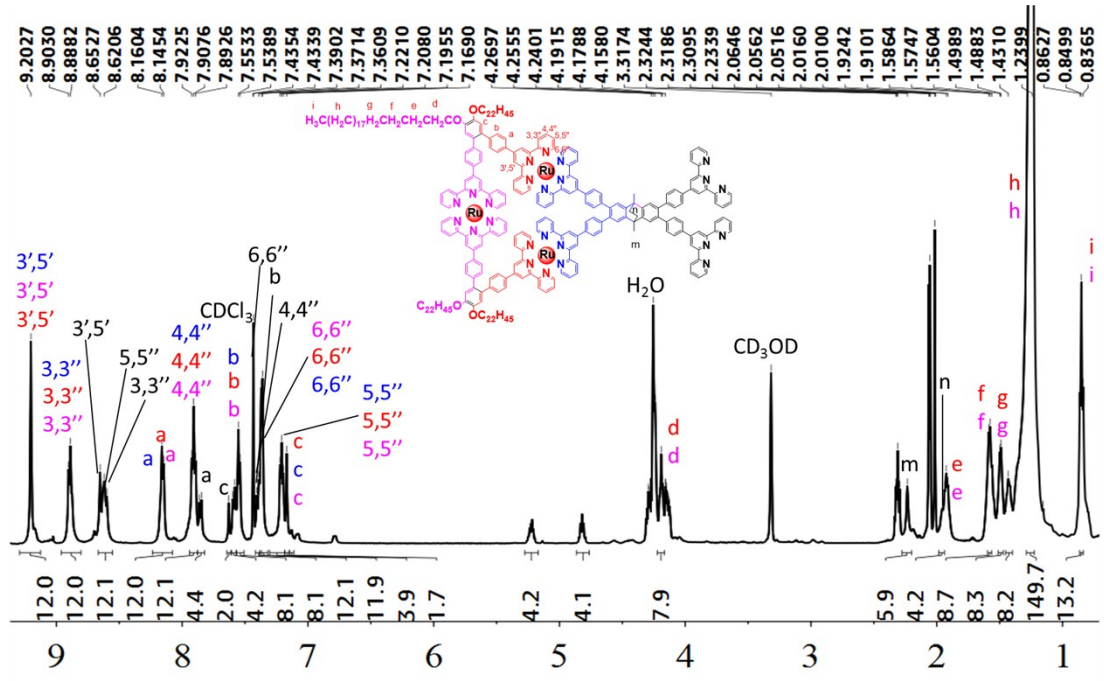

Figure S9. ^{1}H NMR spectrum (500 MHz, 300 K) of **7** in CD_3OD: $CDCl_3$ (1:2, v/v).

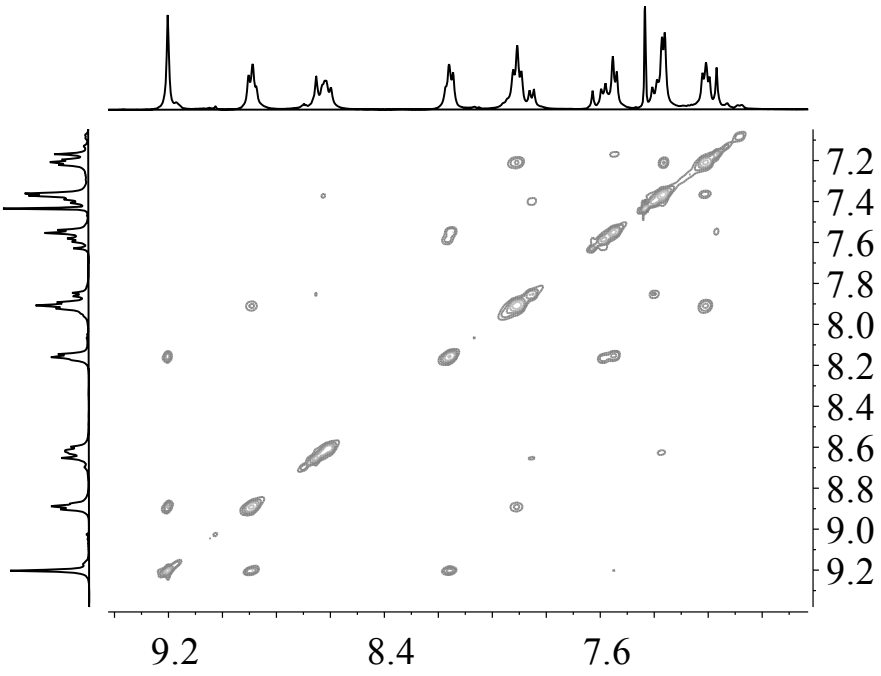

Figure S10. 2D ^{1}H-^{1}H NOESY NMR spectrum (500 MHz, 300 K) of **7** in CD_3OD: $CDCl_3$ (1:2).

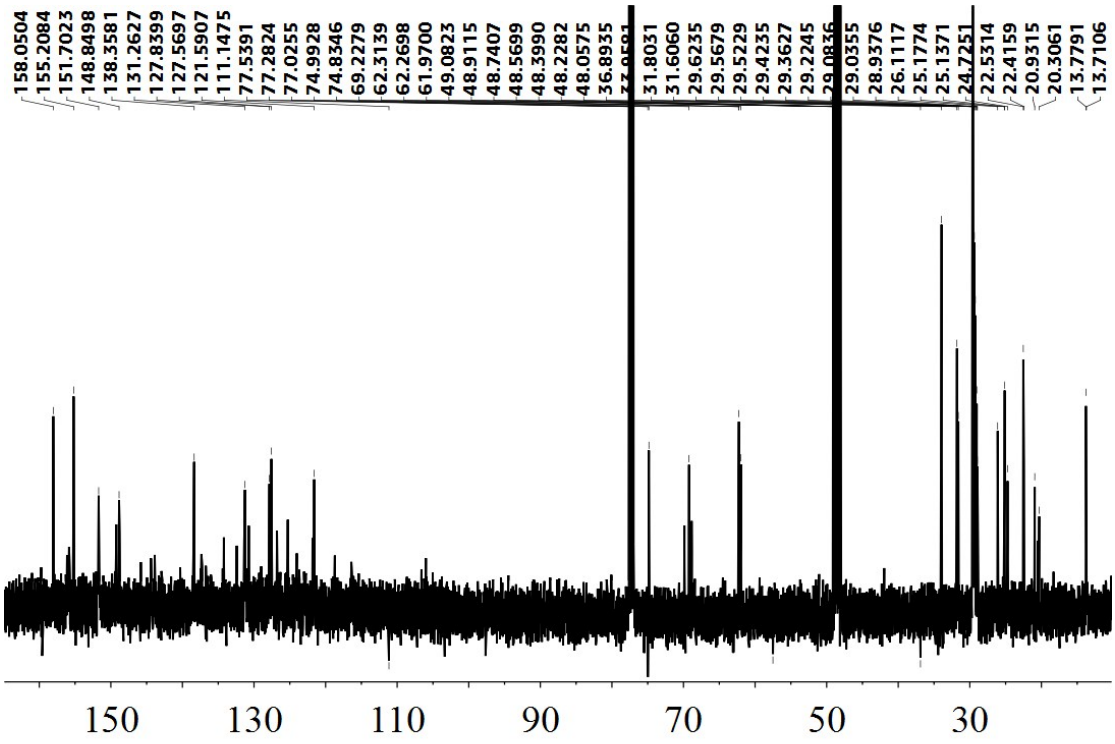

Figure S11. ^{13}C NMR spectrum (500 MHz, 300 K) of **7** in CD_3OD: $CDCl_3$ (1:2).

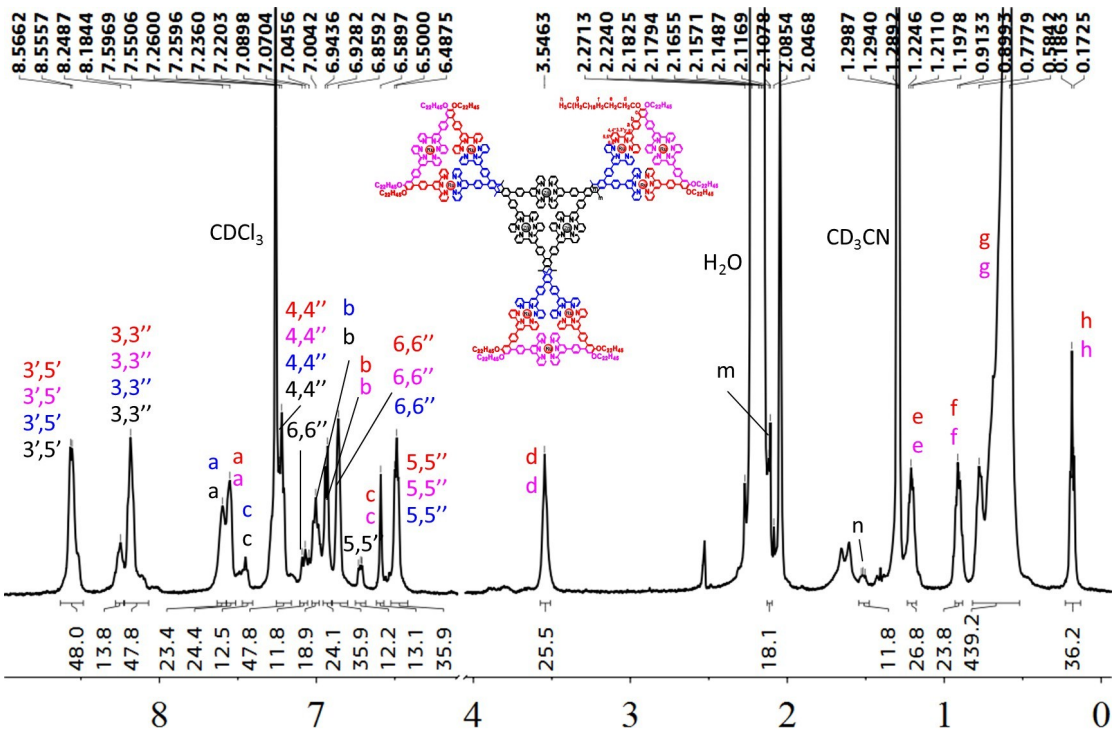

Figure S12. ^{1}H NMR spectrum (500 MHz, 300 K) of **8** (PF_6^-) in CD_3OD: $CDCl_3$ (1:2) and a different solvent system from that in Figure 2).

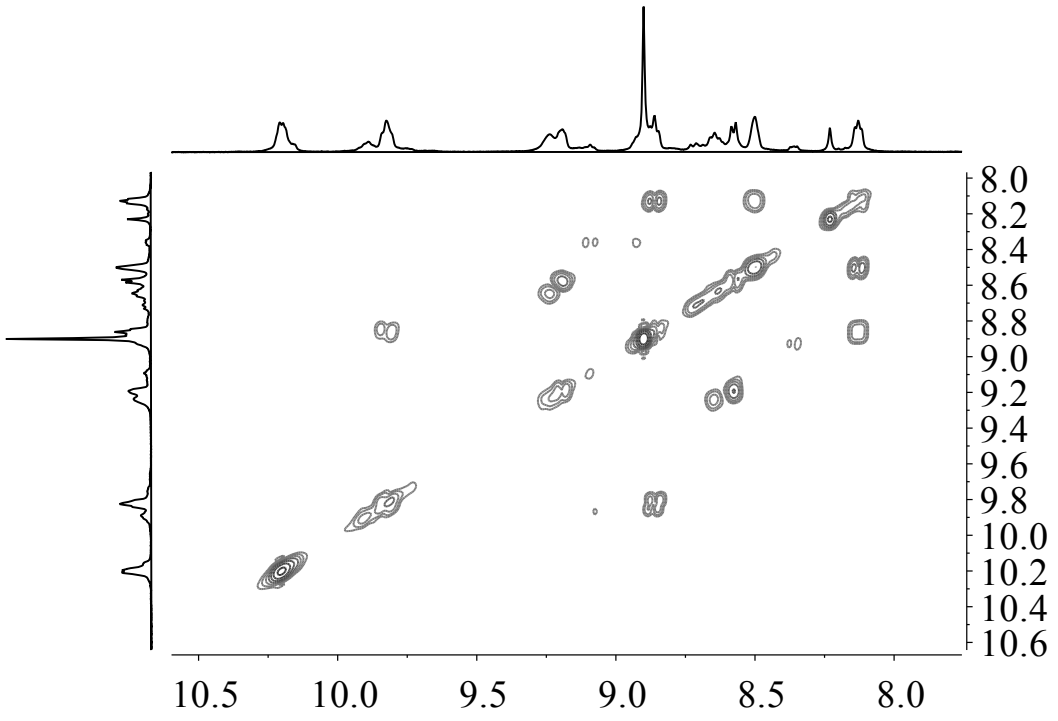

Figure S14. 2D ^{1}H-^{1}H COSY NMR spectrum (500 MHz, 300 K) of **8** (PF_6^-) in 1:2 $CDCl_3$: CD_3CN.

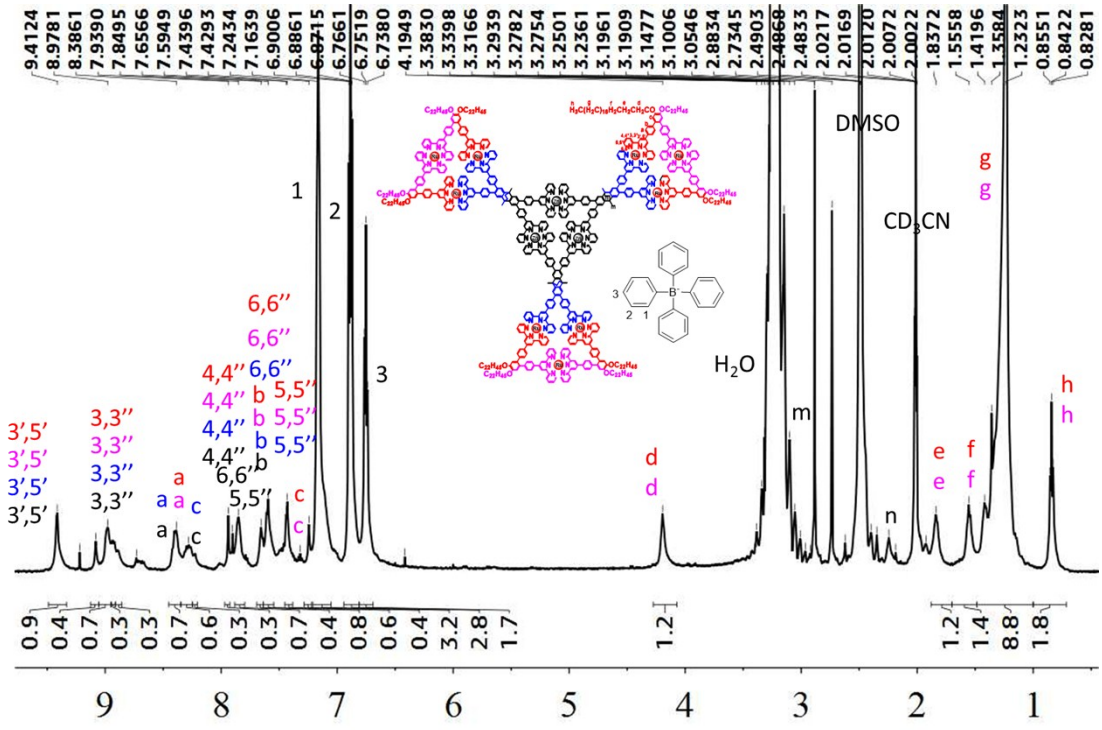

Figure S15. ^{1}H NMR spectrum (500 MHz, 300 K) of **9** (8 BPh_4^-) in 1:4 CD_3CN: DMSO-D_6.

ESI-TWIM-MS, AFM, DLS, and UV-vis results

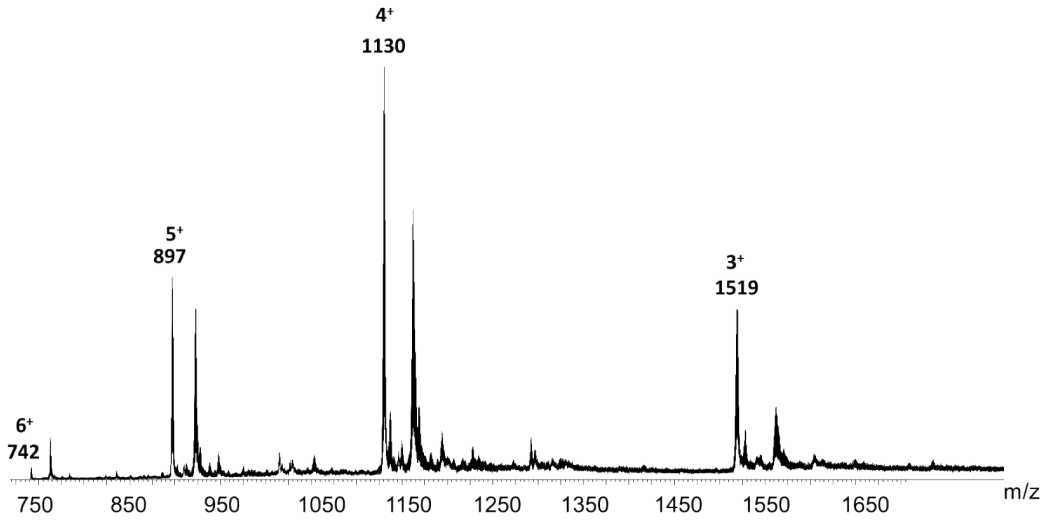

Figure S16. ESI-MS spectrum of **7**.

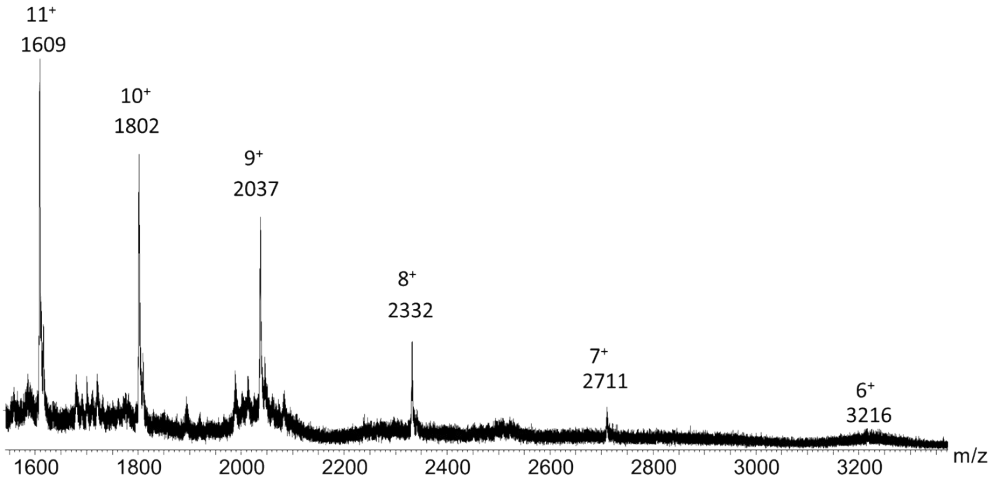

Figure S17. ESI-MS spectrum of **9** (**8** BPh_4^-).

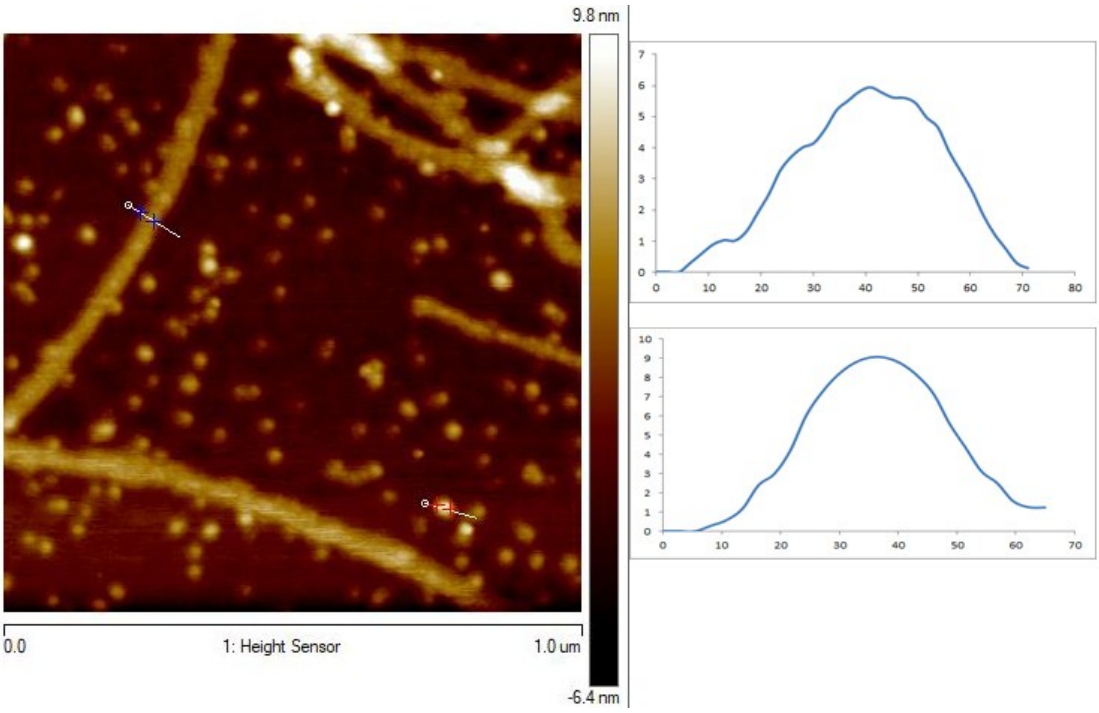

Figure S18. The AFM image of aggregations of complex **8** (PF_6^-).

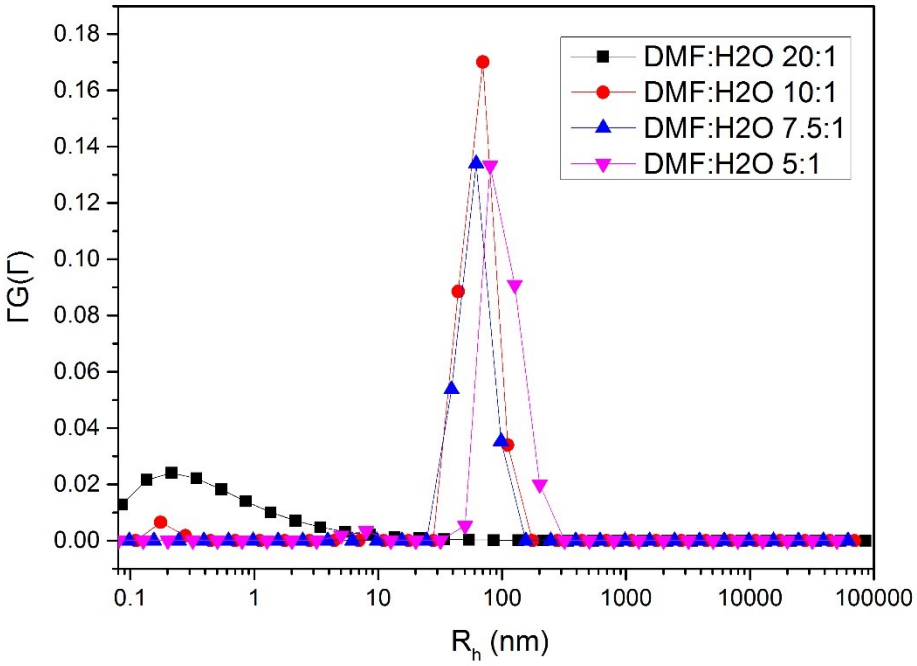

Figure S19. The DLS plots of complex **8** (PF_6^-, 1.2 mg/mL), as continuous addition of H_2O to DMF solution).

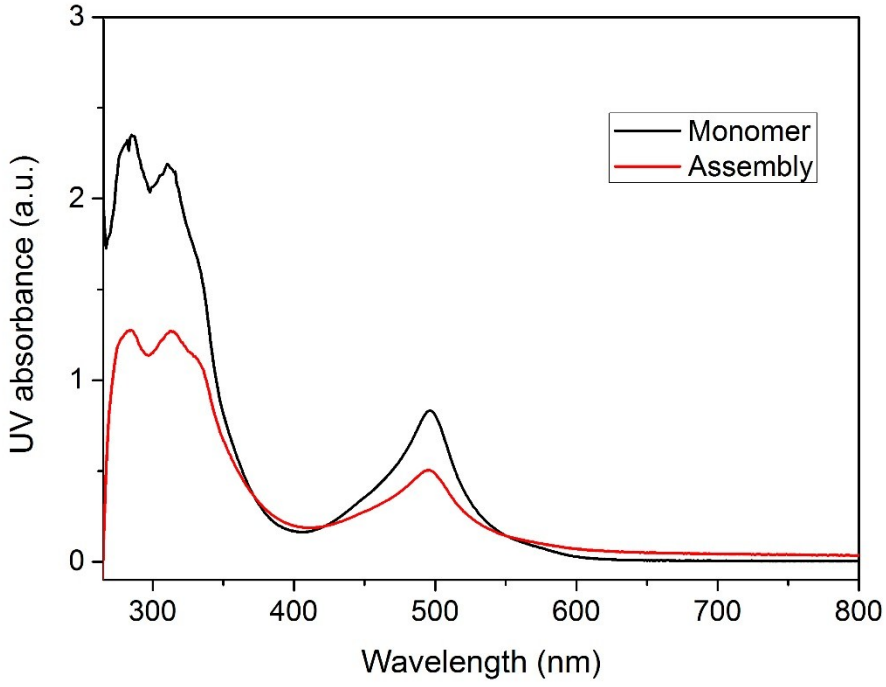

Figure S20. The UV-vis images for the monomer (500 μg/mL, DMF) and assembly [500 μg/mL, DMF : H_2O (5:1, v/v)] of complex **8** (PF_6^-).

References

S1 K. Thalassinos, M. Grabenauer, S. E. Slade, G. R. Hilton, M. T. Bowers and J. H. Scrivens, *Anal. Chem*., 2008, **81**, 248-254.

S2 F. A. Fernandez-Lima, R. C. Blasé and D. H. Russell, *Int. J. Mass Spectrom*., 2010, **298**, 111-118.

S3 P. Jarozs, K. Lotito, J. Schneider, D. Kumaresan, R. Schmehl and R. Eisenberg, *Inorg. Chem*., 2009, **48**, 2420-2428.

S4 S. Chakraborty, R. Sarkar, K. J. Endres, T.-Z. Xie, M. Ghosh, C. N. Moorefield, M. J. Saunders, C. Wesdemiotis and G. R. Newkome, *Eur. J. Org. Chem.,* 2016, 5091-5095.

S5 A. Schultz, X. Li, B. Barkakaty, C. N. Moorefield, C. Wesdemiotis and G. R. Newkome, *J. Am. Chem. Soc.,* 2012, **134**, 7672-7675.

S6 E. Alessio, G. Mestroni, G. Nardin, W. M. Attia, M. Calligaris, G. Sava and S. Zorzet, *Inorg. Chem*., 1998, **27**, 4099-4106.

S7 T.-Z. Xie, K. Guo, Z. Guo, W.-Y. Gao, L. Wojtas, G.-H. Ning, M. Huang, X. Lu, J.-Y. Li, S.-Y. Liao, Y.-S. Chen, C. N. Moorefield, M. J. Saunders, S. Z. D. Cheng, C. Wesdemiotis and G. R. Newkome, *Angew. Chem. Int. Ed*., 2015, **54**, 9224-9229; *Angew. Chem*., 2015, **127**, 9356-9361.